A Unified Approach to the Synchronous Performance Analysis of Single and Poly-Phase Line-Fed Interior Permanent Magnet Motors

Mircea Popescu[1] TJE Miller[1] Malcolm McGilp[1] Calum Cossar[1] Dan Ionel[2] and S.J. Dellinger[3]
1 – SPEED Laboratory, University of Glasgow, U.K.
2 – AO Smith Corporation, Milwaukee, WI, USA
3 – AO Smith Electrical Products, Tipp City, OH, USA

***Abstract* – Interior permanent magnet motors equipped with a squirrel-cage rotor have lately received an increased interest. Defined as line-start, line-fed or hybrid synchronous-induction motors, such machines combine the advantage of the brushless permanent magnet motors, i.e. high efficiency, constant torque for variable speed, with the high starting capability of the induction motors connected directly to the supply system. This paper proposes a unified analysis of these motors, with an emphasis on how any possible configuration may be described by using symmetrical components and two equivalent fictitious machines: positive and negative sequences. The analysis is validated on a single-phase unbalanced motor and on a three-phase balanced line-fed interior permanent magnet motor.**

***Index terms* – interior permanent magnet motors, line-fed, line-start, symmetrical components, balanced operation, flux-MMF diagram**

I. Introduction

The line-fed interior permanent magnet motor (LFIPM) is gaining increased popularity, especially in constant speed variable torque applications, by making possible the achievement of superior efficiency without the additional cost of power electronics. For the optimal design of this type of motor, the ability of calculating and modelling in the equivalent circuit the core losses that directly impact the efficiency and the estimation of the maximum torque (pull out) capability, considering at the full extent the non-linearity of the motor parameters, are both of great importance and yet have received less publication coverage, e.g. [1-6, 10-13]. The present paper aims at filling the gap based on a new method with wide applicability and in the process will cover other aspects of interest such as the identification of the contribution of each of the phases to the motor average torque. A combination of equivalent circuit and finite element calculations are employed and the results validated against a systematic experimental program, which included both single and three-phase motors.

II. General Model of LFIPM Motors

Voltage and torque equations

We will consider the general case of motor with two phases and supplied from an unbalanced system. The transformed d-q axis voltages and currents are linked to the actual values through the relations described in [1]. If the supply voltage is a single-phase sinusoidal source [$v_s = V_S\sqrt{2}\cos\omega t$], for the case of steady-state operation (constant rotor flux) the symmetrical components method will be employed. Then the LFIPM motor performance analysis may be decomposed in two sections: positive and negative sequences. The positive and negative sequence voltages $\mathbf{V}_1$,$\mathbf{V}_2$ depend on the equivalent positive and negative impedances $\mathbf{Z}_1$, $\mathbf{Z}_2$. A good choice for the initial value of $\mathbf{V}_1$ is the supply voltage phasor amplitude $\mathbf{V}_S$. Assuming that the stator windings are magnetically orthogonal we may write:

$$\mathbf{V}_1 = \mathbf{V}_S \cdot \frac{\sqrt{2}}{\beta} \cdot \frac{\beta + j\,\mathbf{a}_2}{\mathbf{a}_1 + \mathbf{a}_2} \tag{1}$$

$$\mathbf{V}_2 = \mathbf{V}_S \cdot \frac{\sqrt{2}}{\beta} \cdot \frac{\beta - j\,\mathbf{a}_1}{\mathbf{a}_1 + \mathbf{a}_2} \tag{2}$$

where β is the effective turns ratio and:

$$\begin{aligned} \mathbf{a}_1 &= 1 - \frac{jX_C}{\mathbf{Z}_1} \cdot \left(1 + j \cdot \frac{1}{\beta}\right) \\ \mathbf{a}_2 &= 1 - \frac{jX_C}{\mathbf{Z}_2} \cdot \left(1 - j \cdot \frac{1}{\beta}\right) \end{aligned} \tag{3}$$

Note that for an unbalanced inverter-fed IPM, where there is no auxiliary capacitive impedance $\mathbf{a}_1 = \mathbf{a}_2 = 1$ and thus:

$$\mathbf{V}_1 = \frac{\mathbf{V}_S}{\beta} \cdot \frac{\beta + j}{\sqrt{2}} \tag{4}$$

$$\mathbf{V}_2 = \frac{\mathbf{V}_S}{\beta} \cdot \frac{\beta - j}{\sqrt{2}} \tag{5}$$

If the positive sequence impedance $\mathbf{Z}_1$ is variable with the load angle δ and will be determined through an iterative process, the negative sequence impedance is averaged for *dq* axes. The method of finding the value of positive sequence impedance is an iterative one [1].

The negative sequence impedance $\mathbf{Z}_2$ is considered constant at synchronous speed and is computed as:

$$\begin{aligned} \mathbf{Z}_2 = R_s + jX_{ls} &+ \frac{1}{2} \cdot \frac{jX_{md} \cdot \left(\frac{R_{rd}}{2} + jX_{lrd}\right)}{\frac{R_{rd}}{2} + j \cdot \left(X_{md} + X_{lrd}\right)} \\ &+ \frac{1}{2} \cdot \frac{jX_{mq} \cdot \left(\frac{R_{rq}}{2} + jX_{lrq}\right)}{\frac{R_{rq}}{2} + j \cdot \left(X_{mq} + X_{lrq}\right)} \end{aligned} \tag{6}$$

The corresponding torques for the positive and negative sequence are computed from the power balance at synchronous angular velocity:

$$T_{e1,2} = \frac{P}{2\omega_s} \cdot \left[\mathrm{Re}\left(\mathbf{V}_{1,2} \cdot \left(\frac{\mathbf{V}_{1,2}}{\mathbf{Z}_{1,2}} \right)^* \right) - R_s \cdot \left| \frac{\mathbf{V}_{1,2}}{\mathbf{Z}_{1,2}} \right|^2 \right] \tag{7}$$

The total electromagnetic torque at steady-state operation will be:

$$T_e = T_{e1} + T_{e2} \tag{8}$$

Equations (7) and (8) provide an original method of estimating the positive and negative sequence voltages and currents. The total average torque (T_e) and the positive sequence torque (T_{e1}) may be directly measured. The negative sequence torque (T_{e2}) will be deduced from (8). The positive and negative sequences impedances are computed with (6) or as described in [1]. Consequently, $\mathbf{V}_1$ and $\mathbf{V}_2$ are extracted by using (7) and may be compared with the computed results (2), (3).

Generally, the analysis of a synchronous permanent magnet motor with salient rotor (e.g. LFIPM motor) is made using the Park transformation. The symmetrical component voltages may be expressed as:

$$\mathbf{V}_1 = V_{d1} + jV_{q1} \tag{9}$$

$$\mathbf{V}_2 = V_{d2} + jV_{q2} \tag{10}$$

In steady-state operation we have the following expressions:

(a) for the positive sequence the rotor bar currents become null (i.e. $I_{dr} = I_{qr} = 0$) such that in d-q axis coordinates the matrix voltage equation is expressed by:

$$\begin{bmatrix} V_{d1} \\ V_{q1} - E_{q11} \end{bmatrix} = \begin{bmatrix} R_s & -X_q \\ X_d & R_s \end{bmatrix} \cdot \begin{bmatrix} I_{d1} \\ I_{q1} \end{bmatrix} \tag{11}$$

(b) for the negative sequence the induced rotor bar currents have a double frequency as referred to the fundamental frequency, such that in *dq* axis coordinates the matrix voltage equation is expressed by:

$$\begin{bmatrix} V_{d2} \\ V_{q2} - E_{q12} \\ 0 \\ 0 \end{bmatrix} = \begin{bmatrix} R_s & -X_q & 0 & -X_{md} \\ X_d & R_s & X_{mq} & 0 \\ 0 & 0 & R_{rd} & 0 \\ 0 & 0 & 0 & R_{rq} \end{bmatrix} \cdot \begin{bmatrix} I_{d2} \\ I_{q2} \\ I_{rd2} \\ I_{rq2} \end{bmatrix} \tag{12}$$

Note that the d-q axis impedances are computed for the synchronous angular velocity (ω_s).

The positive and negative sequence torque components may be further decomposed in alignment (excitation) torque, reluctance torque or cage torque (just for the negative sequence voltage):

$$\begin{aligned} T_e &= T_{rel} + T_m + T_{cage} \\ T_{rel} &= \frac{mP}{2}\left(L_d - L_q\right) I_d I_q \\ T_m &= \frac{mP}{2\omega_s} E_{q1} I_q \\ T_{cage} &= \frac{mP}{2}\left(L_{md} I_{dr} I_q - L_{mq} I_{qr} I_d\right) \end{aligned} \tag{13}$$

where m is the number of phases, P the number of poles, L_d, L_q are the *dq* synchronous inductances, L_{md}, L_{mq} are the magnetizing components of the *dq* synchronous inductances,

The above relations represent the most general case when the stator resistance cannot be neglected and reluctance effect is included. Several simplified cases may be obtained: for the case of large PM synchronous motors usually the stator resistance is neglected ($R_s = 0$), or for an isotropic machine the synchronous d-q axis reactance is the same in both axes ($X_d = X_q = X_s$).

The pull-out torque will correspond to the load angle when the electromagnetic torque computed with (7) is maximum. A simple solution of the derivative of (7) using the torque components from (13) with load angle δ in order to find the maximum value of the torque is not possible, because the inductances vary as well with load angle.

Core loss modeling in LFIPM motors

Similarly to the synchronous motor, in LFIPM motors the stator iron losses occur in the teeth and in the yoke. The loss is a function of the total flux in the teeth and in the yoke. If we consider that the yoke and most of the teeth carry a flux which is proportional to the stator flux linkage, it appears to be appropriate to connect an equivalent iron loss resistance (R_c) either at the terminals of the motor equivalent circuit, or more correctly inside the stator resistance R_s where the voltage across R_c would be the total induced voltage in the stator winding. Thus, the equivalent L *d-q* axis circuit in Fig. 1 [3] may be employed for both positive and negative sequences with the appropriate voltages. It should be emphasised that the equivalent iron loss resistance R_c exhibits different values with frequency variation or with current (load) and voltage variation (through saturation effect). Also, test data allows the extraction of the sum between iron loss and stray load losses. Even tests performed at no-load operation will give only an estimation for the iron loss. Thus R_c is usually computed either empirically using empirical coefficients or finite element analysis.

The mechanical loss is not controllable through electromagnetic design, but the copper loss and iron loss can be minimised either through an optimised design or more expensively through an optimised control strategy (e.g., vector control). If we consider that the total iron loss may be separated into those caused by mutual flux and called iron loss and those caused by the leakage flux and called stray-load loss, the equivalent circuit (T *d-q* axis) in Fig. 2 has to be used [2]. The mutual flux is comprised of magnet flux and flux created by stator current (armature reaction flux). This flux is proportional to the internal or air gap voltage. It follows that a resistor connected across the air gap voltage can represent the iron-loss. For similar reasons, a resistor $R_{s\text{-}l}$ placed across the leakage reactance ωL_{ls} will represent the stray-load losses. Stray-load losses are comprised of several complex components, not just iron-loss due to the leakage flux. Their physical causes are still under debate.

Another approach is to simulate the iron loss components with two equivalent resistors: one that denotes the voltage dependent losses (similar to a conventional synchronous machine) and one that denotes the current dependent losses. The resistor placed in parallel with the total induced voltage depends on the leakage and magnetization fluxes. This would be similar to the equivalent circuit in Fig. 1, but with the difference that R_c takes into account only the so-called voltage dependent iron loss. Actually, the induced voltage due to the magnets determines these losses. The resultant equivalent circuit Ti *d-q* axis) is illustrated in Fig. 3 [4]. For all models, the voltage and torque equations are modified accordingly to accommodate the core loss resistances. All the above equivalent circuits may be used for the synchronous motor dynamic and steady-state operation analysis. Note that as at steady-state the synchronous motor operates like a DC machine, the terms $L\left(di/dt\right)$ are zero.

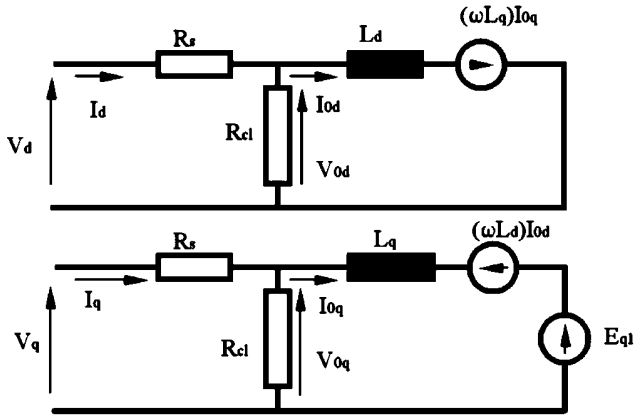

Fig. 1 Equivalent L d-q axis circuit including core losses

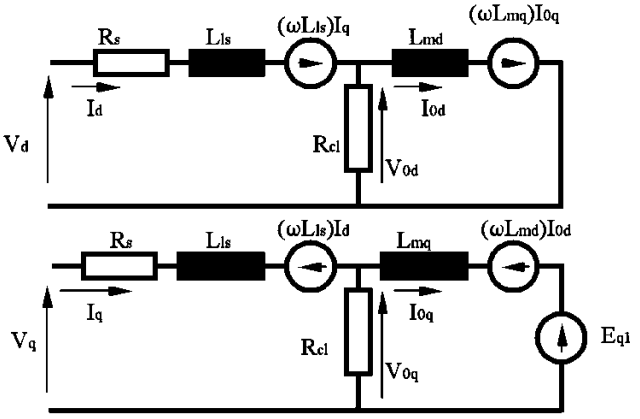

Fig. 2 Equivalent T d-q axis circuit including core losses

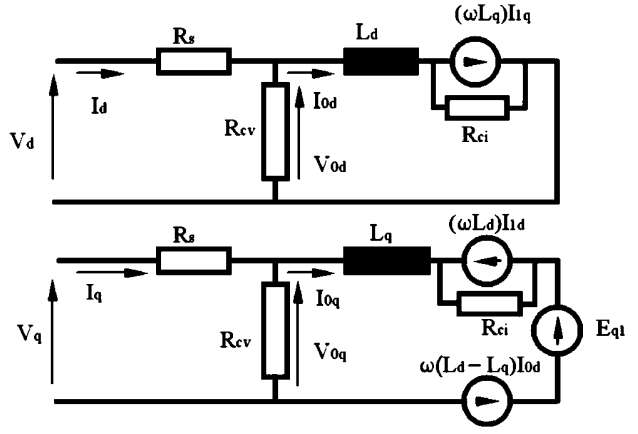

Fig.3 Equivalent L from Ti d-q axis circuit including core losses

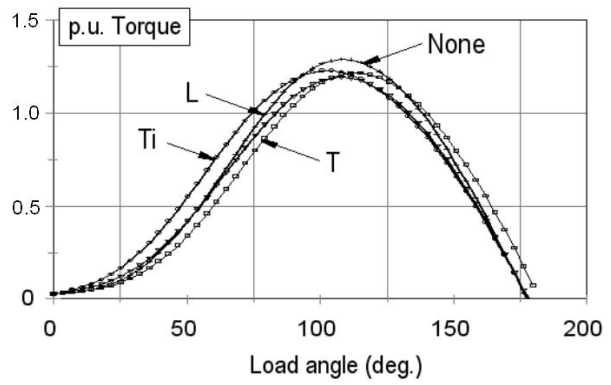

Fig.4 Illustrative LFIPM motor torque variation with load angle when iron loss effect is included

Fig. 4 illustrates the average torque variation with load angle for the LFIPM motor when different equivalent circuits are employed. Note that (a) the equivalent circuit described in Fig. 1 predicts a lower electromagnetic torque value for the whole range of load angle; (b) the equivalent circuit described in Fig. 2 predicts a lower electromagnetic torque value for the load angle variation between zero and the load angle corresponding to maximum torque; (c) the equivalent circuit described in Fig. 2 predicts a higher electromagnetic torque value for the load angle variation between the load angle corresponding to maximum torque and maximum load angle; (d) the equivalent circuit described in Fig. 3 predicts a higher electromagnetic torque value for the load angle variation between zero and the load angle corresponding to maximum torque; (e) the equivalent circuit described in Figs. 3 predicts a lower electromagnetic torque value for the load angle variation between the load angle corresponding to maximum torque and maximum load angle; (f) all the equivalent circuits that include iron loss effects predict a lower maximum electromagnetic torque compared to the case when the iron losses are neglected.

Equivalent circuit parameter estimation

An accurate computation of the LFIPM motor parameters requires a combination of analytical and numerical methods. Generally, the synchronous performance of a LFIPM motor can be computed using values of the synchronous inductances L_d and L_q, and of the magnet flux-linkage, which are strongly affected by saturation but which remain independent of rotor position [7–9]. There are cases of IPM motors in which L_q can vary by as much as 5:1 between no-load and full-load, while the *q*-axis flux can saturate the pole-pieces and the stator teeth to such an extent that the effective magnet flux-linkage is also affected. Such cases are ideally characterized by constant values of I_d, I_q, ψ_d and ψ_q throughout the electrical cycle.

If L_d, L_q and the magnet flux-linkage also remain constant throughout the cycle, it suffices to calculate these parameters at only one instant during the cycle [9]. L_d and L_q are both affected by saturation. To some extent, L_d is a function of I_q, and L_q is a function of I_d, because of "cross-saturation". The magnet flux is also affected by saturation, notably by the saturation caused by I_q when $I_d = 0$. Note that the usage of fixed value inductances in computing the electromagnetic torque components (13) may lead to important errors. The inductance values are usually obtained using a series of finite-element computations using a minimal number of solutions [9].

Fig. 5 shows a cross-section with flux-lines plot for a LFIPM motor, while Figs. 6 and 7 show the variation pattern of the *dq* axis inductances vs and current and load angle, δ.

The computation burden can be reduced by using curve fitting-methods to estimate the inductance at points where we do not have a finite-element result. The *dq* axes inductances are computed considering just the fundamental harmonic of the phase flux-linkage waveforms.

A strong MMF harmonic content may lead to another source of errors in the computation of L_d and L_q and further in the average torque computation. The magnet flux and the back EMF, E_{q1} are also variable with current amplitude and the torque angle γ.

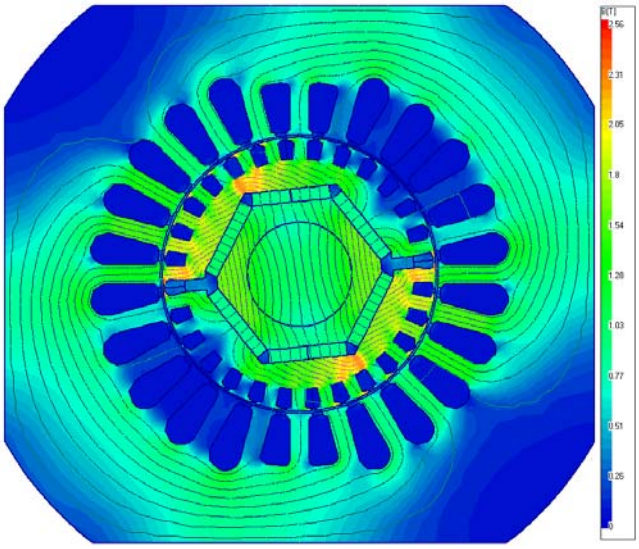

Fig. 5 Cross-section with flux-lines plot of a LFIPM

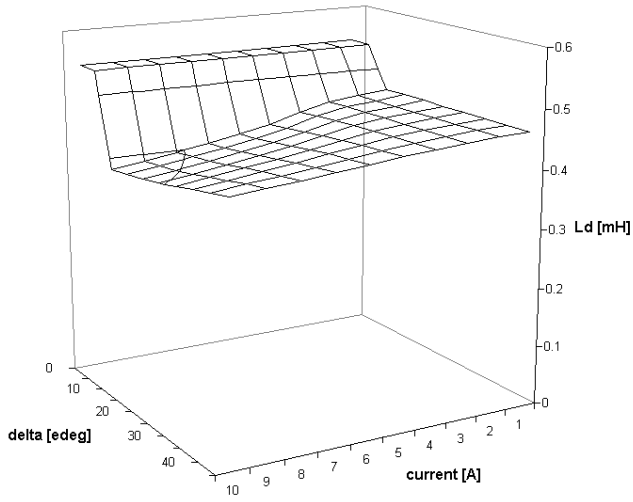

Fig. 6 L_d variation under load conditions

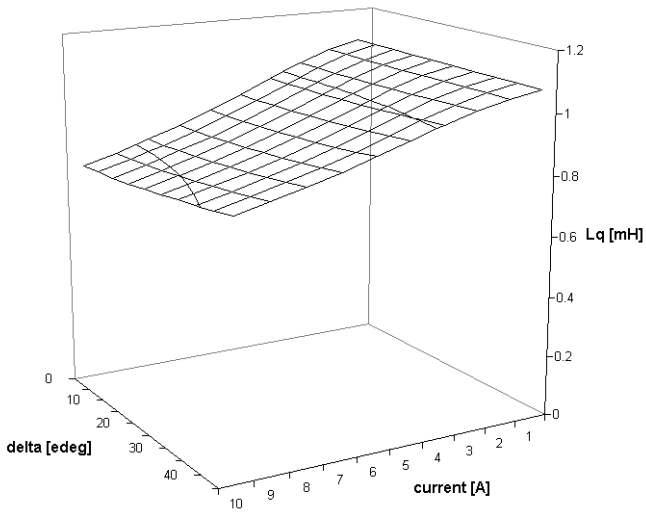

Fig. 7 L_q variation under load conditions

However, it is impossible to measure the back EMF under load conditions. Thus, even though the system is non-linear, the superposition principle is applied to compute the magnet flux and consequently the back EMF. The core loss resistance R_C will vary with frequency and load conditions, i.e. currents. Once the motor parameters are known, by using (7-13) we can compute the average resultant electromagnetic torque.

For an unbalanced two-phase LFIPM motor we note that: (a) the positive sequence produces the dominant torque component; (b) there is only one balanced operation point, when the negative sequence torque is zero; (c) the variable rotor reluctance generally has a low contribution to the resultant torque and usually the pull-out torque is determined by the maximum alignment torque of the positive sequence.

III. Computations and Experimental Validation

The validation of the average electromagnetic torque values obtained with (6-11) is done through the usage of the flux-MMF diagram [8-9]. In the finite-element problem we use as sources the actual phase currents that are sinusoidal in a LFIPM motor. In a two-phase motor, the contribution of the each phase to the torque production is different whereas in the case of a balanced supply voltage system (2 or 3 phase) all phases will contribute with the same amount of energy to the resultant average torque.

For experimental validation two LFIPM motors are employed: one motor with two unsymmetrical windings and one balanced 3-phase wye connected motor. Both motors are rated as 2-pole, 230V, 5HP. The motor parameters are listed in the Appendix.

Unbalanced LFIPM

Figs. 8 and 9 show the computed flux-MMF loops for the unbalanced 2-phase motor and the equivalent 2-phase balanced tested motors under load conditions with sinewave currents. The amplitude of main winding current is 5.9A in both cases. The auxiliary winding current is leading by 90 edeg the main winding current in both cases and has an amplitude of 4A for the unbalanced motor and 8A for the balanced 2-phase motor.

The equivalent 2-phase balanced motor was obtained by imposing a current ratio I_a / I_m equal to the effective turns ratio main / auxiliary, i.e. 1.34. Thus, the phase MMFs are identical.

Note that for the unbalanced 2-phase motor the main phase produces about 70% of the total average torque while the auxiliary phase contributes only 30% of the total torque.

The difference between the torque that is produced by the equivalent 2-phase balanced motor and the actual unbalanced 2-phase motors will give the negative sequence torque. For the analysed case, the balanced motor will produce an electromagnetic torque of T_{e1} = 25.66lb-in, while the actual unbalanced motor produces an electromagnetic torque of T_e = 19.11lb-in. Consequently, the corresponding negative sequence torque is estimated as T_{e2} = 6.55lb-in.

A similar result is obtained through static measurements and computations. The two stator-windings are supplied with DC currents equal with the amplitude of the AC currents employed for Figs. 8-9. The rotor position is changed incrementally for a cycle of 360 electrical degrees and the electromagnetic torque is recorded.

For a complete description of the procedure several tests are performed: both main and auxiliary windings are energized, only the main or the auxiliary winding is energized.

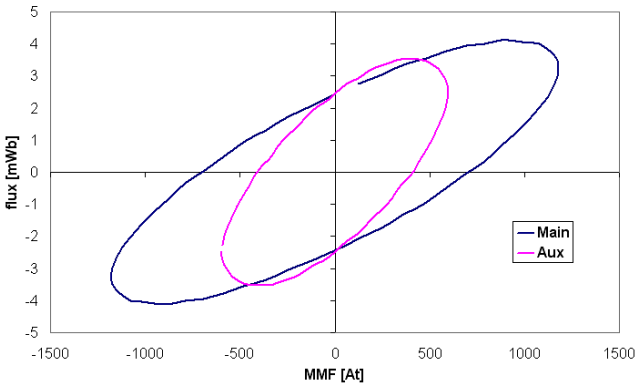

Fig. 8. Flux-MMF diagram – unbalanced LFIPM motor

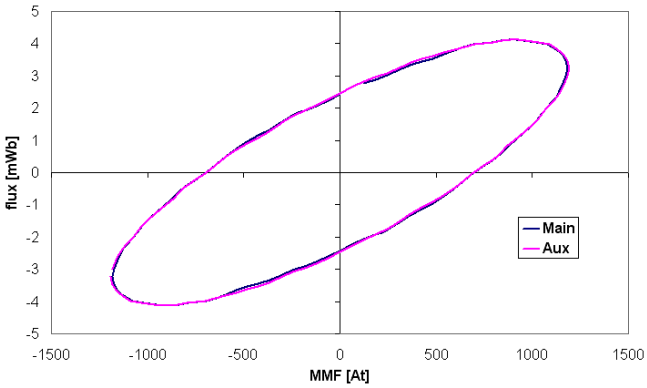

Fig. 9. Flux-MMF diagram – balanced LFIPM motor

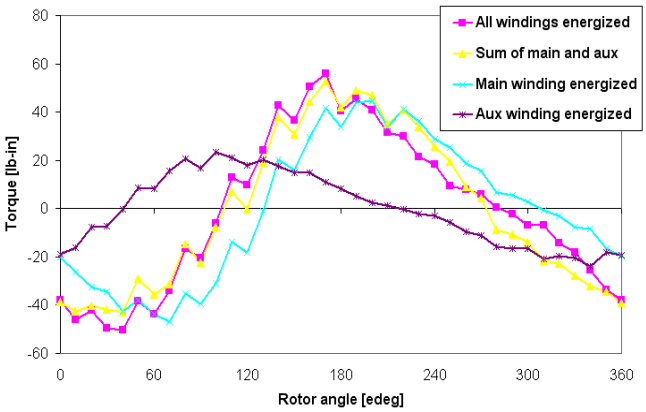

Fig. 10. Static torque measurements – unbalanced LFIPM motor

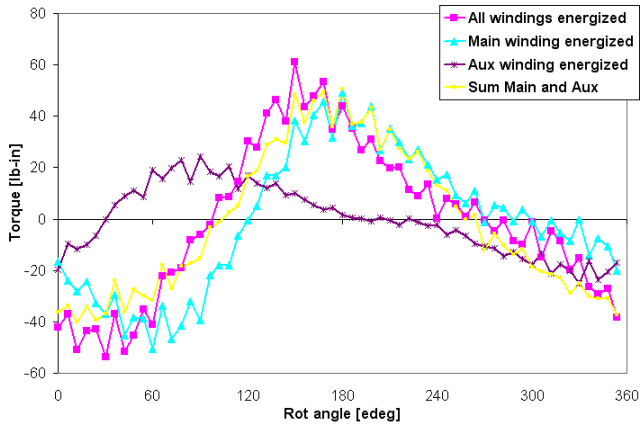

Fig. 11 Static torque calculations – unbalanced LFIPM motor

Figs. 10 and 12 show the measured static torque for the unbalanced and balanced motor respectively.

Figs. 11 and 13 show the finite-element computed results for the static torque.

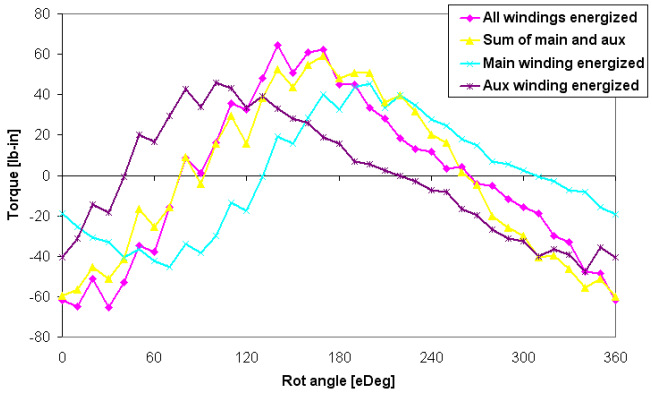

Fig. 12 Static torque measurements – balanced LFIPM motor

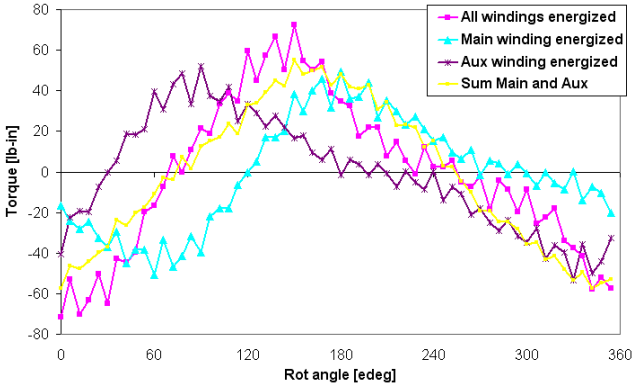

Fig. 13 Static torque calculations – balanced LFIPM motor

We note the following:

– The application of the superposition principle may be considered as acceptable if we compare the total measured static torque with the sum of the torques that are produced when only one winding is energized;

– The motor torque capability for a certain current level may be extracted from the static torque results.

– The effect of the induced rotor bar currents by the negative sequence voltage is ignored

The negative sequence torque is given by the difference between the total torque measured or computed for the unbalanced motor (Figs. 10-11) and the total torque measured or computed for the balanced motor torque (Figs. 12-13).

At each load angle – that will correspond to the rotor angle in static tests – we can identify the negative sequence torque variation (Fig. 14). By using the torque waveform for the balanced motor we associate the first rotor position for which the torque is zero, i.e. 65 edeg with a load angle $\delta = 0$ edeg. Thus, for the tested motor we can estimate a negative sequence torque that exhibits a maximum value of approximately 30% of the maximum positive sequence torque.

The negative sequence torque waveform is advanced with 20 edeg as compared to the positive sequence torque waveform.

Obviously, in a capacitor motor the stator currents will vary with the load angle when the voltage is imposed and the shift angle between the current phasors will vary also. Nevertheless, the static tests provide a better understanding of the motor operation under unbalanced conditions and a satisfactory estimation of the maximum negative sequence torque for a certain current level when the LFIPM is inverter-fed and not directly connected to the voltage supply, i.e. line-start motor type.

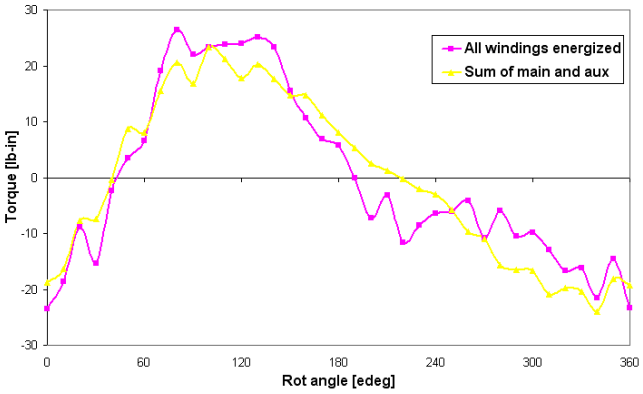

Fig. 14 Static negative sequence torque – unbalanced LFIPM motor

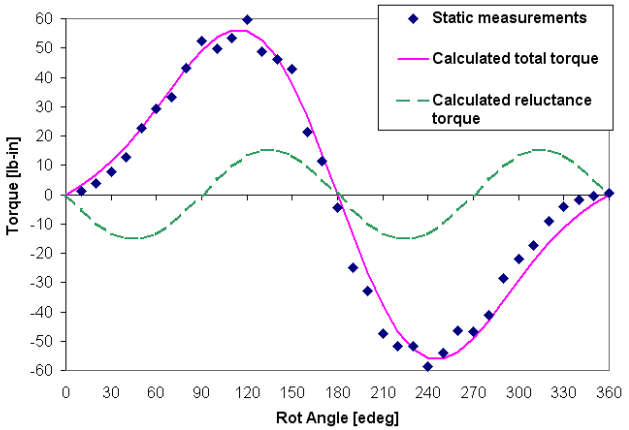

Fig. 15 Static torque measurements and calculations – balanced 3-phase LFIPM

Balanced LFIPM

The analysis of the balanced LFIPM allows a separation of the torque components as per relation (13).

Fig. 15 shows a comparison between the static measurements and the calculated total electromagnetic torque for a 3-phase wye connected LFIPM. Again, for the computed torque components it is assumed that the superposition principle may be applied even though the motor is a non-linear system. The synchronous reactances are computed as described in Section II and measured for a current level of 20A. The inductance measurement was performed on a LFIPM with the cage end-rings removed. The core loss is modeled using the equivalent circuit from Fig. 2.

The rotor angle may be associated with the torque angle, i.e. the angle between the current phasor and the back EMF phasor. With reference to Fig. 15, rotor angle = 90 corresponds to the zero torque angle [8].

The reluctance torque component can be clearly estimated using the measured or estimated synchronous inductances.

IV. Conclusions

The line-fed interior permanent magnet motor may be analysed in a unified approach using the symmetrical components method and two-axis (*dq*) theory. The symmetrical components allow for the treatment of the stator unbalances, i.e. supply voltage or unsymmetrical windings. The two-axis theory allows for the treatment of the salient rotor equipped with magnets and unsymmetrical rotor cage. This analysis is applicable regardless of the number of phases. The prediction of the motor performance can be made using the superposition principle, even though the motor is a non-linear system. A validation of the effect of positive and negative sequence voltage is done through static torque measurements. The equivalent circuit parameters need to be computed for each load point and may be validated with measurements on an equivalent balanced LFIPM motor.

Appendix

MOTOR PARAMETERS

Line-fed permanent-magnet AC motors: 2-pole, 230 V, 5HP

Motor	2-phase unbalanced	3-phase balanced
R_m. [ohms]	1.58	0.115
R_a [ohms]	1.48	N/A
L_d [mH]	102	4.80
L_q [mH]	124	8.00
E_0 [Vrms]	215	63.5
f [Hz]	60	120

References

[1]. Miller TJE, Popescu M, Cossar C, McGilp MI, Strappazzon G, Trivillin N, Santarossa R. – "Line Start Permanent Magnet Motor: Single-Phase Steady-State Performance Analysis" – *IEEE Trans. on Ind. Appl.* – Vol. 40, No. 2, March/April 2004, pp. 516 – 525

[2]. Honsinger, V.B. "Performance of polyphase permanent magnet machines", *IEEE Trans. Power Appl. Syst.*, vol. PAS-99, pp.1510-1518, July 1980

[3]. Sebastian, T., Slemon, G.R., Rahman, M.A.: "Modeling of permanent magnet synchronous motors", *IEEE Trans. Magnetics*, Vol. MAG –22, No.:5, pp. 1069 – 1071, Sept. 1986.

[4]. Consoli,A., Racitti, A. "Analysis of permanent magnet synchronous motors", *IEEE Trans. on Ind. Appl*, Volume:27, No: 2, March/April. 1991, pp. 350 – 354

[5]. Rahman, M.A.; Osheiba, A.M. "Performance of large line-start permanent magnet synchronous motors", *IEEE Transactions on En. Conv.*, Vol. 5, pp. 211-217, March 1990

[6]. Knight, A.M.; McClay, C.I. "The design of high-efficiency line-start motors" *IEEE Trans. on Ind. Appl*, Volume: 36 Issue: 6 , pp: 1555 –1562, Nov.-Dec. 2000

[7]. Nee, H.-P.; Lefevre, L.; Thelin, P.; Soulard, J. "Determination of d and q reactances of permanent-magnet synchronous motors without measurements of the rotor position" *IEEE Trans. on Ind. Appl* , Volume: 36 Issue: 5 , Sept.-Oct. 2000, Page(s): 1330 –1335

[8]. Miller TJE, Popescu M, Cossar C, McGilp MI: "Performance Estimation of Interior Permanent-Magnet Brushless Motors Using the Voltage-Driven Flux-MMF Diagram" –*IEEE Transactions on Magnetics*. – Vol. 42, No. 7, July 2006, pp. 1867-1873

[9]. Miller TJE, Popescu M., Cossar C., Mcgilp M.I., Olaru M., Davies A.J., Sturgess J.P., Sitzia A.M. "Embedded Finite-element Solver for Computation of Permanent-Magnet Brushless Motors" *IEEE IAS Annual Meeting, Conf. Rec.*, Vol. 3, Oct. 2006, Tampa, FL, pp:1478 – 1485

[10]. Miller, TJE "Single-phase permanent magnet motor analysis", *IEEE Trans. Ind. Appl.*, Vol. IA-21, pp. 651-658, May-June 1985

[11]. Williamson, S.; Knight, A.M. "Performance of skewed single-phase line-start permanent magnet motors" *IEEE Transactions on Ind. Appl.* , Vol. 35, pp. 577 –582, May-June 1999

[12]. Boldea, I., Dumitrescu, T., Nasar, S. "Unified analysis of 1-phase AC motors having capacitors in auxiliary windings" *IEEE Transactions on En. Conversion*, Vol. 14, No.3, September 1999, pp. 577-582

[13]. Sano T., Nakayama E., Sawa K. A study on the electric and magnetic circuit of single phase line start permanent magnet motor"; *Conf. Rec. IEEEE IECON* 2005, pp. 1562-1568

[14]. Miller TJE, McGilp MI, Olaru M. "PC-FEA 5.5 for Windows – Software", SPEED Laboratory, University of Glasgow, Glasgow (UK), 2006

[15]. Miller TJE and McGilp MI, "PC-BDC 7.0 for Windows – Software", SPEED Laboratory, University of Glasgow, Glasgow (UK), 2006